Measurement of transverse spin-relaxation rates in a rubidium vapor by use of spin-noise spectroscopy

G. E. Katsoprinakis, A. T. Dellis, and I. K. Kominis*

[1]*Department of Physics, University of Crete, Heraklion 71103, Greece*
and Institute of Electronic Structure & Laser, Foundation for Research and Technology, Heraklion 71110, Greece
(Received 29 January 2007; published 12 April 2007)

Spin noise sets fundamental limits to the attainable precision of measurements using spin-polarized atomic vapors and therefore merits a careful study. On the other hand, it has been recently shown that spin noise contains useful physical information about the atomic system, otherwise accessible via magnetic-resonance-type experiments. We here show in yet another manifestation of the fluctuation-dissipation theorem, that spin noise reveals information on the spin-coherence dissipation properties of the atomic system, described by $1/T_2$, the transverse spin-relaxation rate. We present the high-resolution measurements of spin noise at a low magnetic field, leading to an accurate comparison of the extracted relaxation rates with the ones inferred from traditional magnetic-resonance-type measurements in optical pumping experiments.

PACS number(s): 32.80.Bx, 31.70.Hq, 32.30.Dx

I. INTRODUCTION

Quantum noise in atomic systems is usually considered to pose an unavoidable fundamental limitation to the achievable measurement precision leading to the so-called standard quantum limits [1]. Spin noise, in particular, limits the attainable precision of measurements involving an ensemble of uncorrelated paramagnetic atoms [2–7] as well as other two-level systems employed, for example, in atomic clocks [8]. Furthermore, the understanding of spin noise of uncorrelated atomic ensembles is crucial for the realization of methods aimed at producing spin squeezing [9–11]. For these reasons it appears essential to directly study spin noise and its various manifestations. However, another important aspect of spin noise is that it can reveal physical properties of the atomic medium under study without the necessity of a specific state preparation usually performed in traditional spectroscopic investigations. In particular, the spin-coherence dissipation properties of a thermal atomic vapor, usually described by the transverse spin-relaxation rate $1/T_2$, can be elucidated by detecting spontaneous spin fluctuations of the atoms, reminiscent of the fundamental fluctuation-dissipation theorem [12].

Historically, spin noise of an ensemble of nuclear spins has been alluded to by Bloch [13] since the early work on nuclear magnetic resonance, and detected later on using a dc SQUID [14]. More recently, nuclear spin-noise imaging [15] has been used as a noninvasive form of magnetic imaging. In a similar fashion, electron spin fluctuations have been detected in an absorption measurement [16] of spontaneous noise spectroscopy of an alkali-metal vapor. A similar dispersion-like measurement [17] has been recently performed [18,19] and used to reveal spectroscopic information in a nondestructive way. Spontaneous spin fluctuations were specifically measured by the corresponding fluctuations they induced in the Faraday rotation angle of a far-detuned probe laser beam. Similar experiments have been carried out in few-spin systems, such as the inference of the relaxation

properties of a single spin system from noise currents in scanning tunneling microscope (STM) noise spectroscopy [20] and in solid-state systems, such as the measurement of electron spin-relaxation times in bulk GaAs [21].

In this work we will present high-resolution measurements of spin noise in a rubidium vapor at low magnetic field. From the spin-noise spectra we extract the transverse spin-relaxation rate $1/T_2$ and compare with the known rates measured in traditional magnetic-resonance-type experiments using intentionally spin-polarized alkali-metal vapors and radio-frequency magnetic fields. This is the first, to our knowledge, experimental demonstration of the fluctuation-dissipation theorem in an atomic spin system. An equivalent geometric picture of this particular manifestation of the fluctuation-dissipation theorem is that the quantum fluctuations of an otherwise spherical normal velocity surface [22] reveal the relaxation properties of the atomic medium in a nonperturbative way. The physical system we use for our measurements is a rubidium vapor in the presence of nitrogen buffer gas and a static magnetic field, interacting with a far-detuned probe laser. The transverse spin-relaxation rate is deduced from the width of the power spectrum of the Faraday rotation angle fluctuations induced by spin noise on the polarization of the probe laser. In Sec. II we will lay out the theoretical description of spin noise, using the formalism of quantum state diffusion [23]. We find this description to be transparent and intuitive, since it directly leads to a stochastic process describing the measured expectation value of the transverse spin. In Sec. III we describe the experimental measurements made followed by their analysis in Sec. IV.

II. THEORETICAL DESCRIPTION OF SPIN NOISE AND ITS MEASUREMENT

A. Stochastic evolution of the transverse spin polarization

For the case of an alkali-metal vapor in the presence of a static magnetic field only, that is, without any optical pumping light or radio-frequency magnetic fields, the atoms are described by a ground state density matrix, the evolution of which is given by [24]

*Electronic address: ikominis@iesl.forth.gr

$$\frac{d\rho}{dt} = -i[\mathcal{H}_g, \rho] + \frac{1}{T_2}\left(s_z \rho s_z - \frac{3}{4}\rho + \frac{1}{2}s_+ \rho s_- + \frac{1}{2}s_- \rho s_+\right),$$

(1)

where $1/T_2 = 1/T_{se} + 1/T_{sd}$ is the transverse spin relaxation rate, with $1/T_{se}$ being the relaxation rate due to alkali-metal–alkali-metal spin-exchange collisions, and $1/T_{sd}$ the relaxation rate due to alkali-metal–alkali-metal and alkali-metal–buffer-gas spin-destruction collisions. Using the identities ($\hbar = 1$)

$$3/4 = s^2 = s_x^2 + s_y^2 + s_z^2 = \frac{1}{2}(s_+ s_- + s_- s_+) + s_z^2,$$

(2)

we can write Eq. (1) in the Lindblad form,

$$\frac{d\rho}{dt} = -i[\mathcal{H}_g, \rho] + \sum_{j=1}^{3}\left(L_j \rho L_j^\dagger - \frac{1}{2}L_j^\dagger L_j \rho - \frac{1}{2}\rho L_j^\dagger L_j\right),$$

(3)

with the three Lindblad operators being

$$L_1 = \frac{1}{\sqrt{2T_2}}s_+, \quad L_2 = \frac{1}{\sqrt{2T_2}}s_-, \quad L_3 = \frac{1}{\sqrt{T_2}}s_z.$$

(4)

When the density matrix evolution is described by the Lindblad equation, it can be shown [25] that the differential change of a quantum state $|\psi\rangle$ after the elapse of a time interval dt is given by the quantum state diffusion equation

$$|d\psi\rangle = -idt\mathcal{H}_g|\psi\rangle + \sum_{j=1}^{3}\left(\langle L_j^\dagger\rangle_\psi L_j - \frac{1}{2}\langle L_j^\dagger\rangle_\psi\langle L_j\rangle_\psi - \frac{1}{2}L_j^\dagger L_j\right)$$

$$\times|\psi\rangle dt + \sum_{j=1}^{3}(L_j - \langle L_j\rangle_\psi)|\psi\rangle d\xi_j,$$

(5)

where the first term represents the Hamiltonian evolution, the second the deterministic drift (dissipation in this case), and the third the stochastic fluctuations, which necessarily accompany the dissipative process. In the above equation, the expectation values of the Lindblad operators are evaluated in the state $|\psi\rangle$. The statistically independent complex stochastic differentials $d\xi_j$, with $j=1,2,3$, satisfy $M(d\xi_i d\xi_j^*) = \delta_{ij}dt$ and $M(d\xi_i d\xi_j) = 0$, where $M(x)$ represents the mean over all possible realizations of the stochastic variable x. To calculate the stochastic fluctuations of $\langle s_+\rangle$, which is the measured observable as will be shown in the following section, we first note that the transverse spin can be written as

$$s_+ = -\sqrt{2}\sum_{F,F'}\lambda_{FF'}T_1^1(FF'),$$

(6)

where

$$T_M^L(FF') = \sum_\mu |F\mu\rangle\langle F'\mu - M|(-1)^{\mu+F}\sqrt{2L+1}$$

$$\times \begin{pmatrix} F & F' & L \\ \mu & M-\mu & -M \end{pmatrix}$$

(7)

are the rank-L irreducible spherical tensor operators, and the coefficients $\lambda_{FF'}$ are given in Table I with $a = I+1/2$ and $b = I-1/2$ denoting the upper and lower hyperfine multiplet,

TABLE I. Coefficients $\lambda_{FF'}$.

F/F'	a	b
a	$\sqrt{\dfrac{(I+1)(2I+3)}{6(2I+1)}}$	$-\sqrt{\dfrac{2I(I+1)}{3(2I+1)}}$
b	$\sqrt{\dfrac{2I(I+1)}{3(2I+1)}}$	$-\sqrt{\dfrac{I(2I-1)}{6(2I+1)}}$

respectively. For brevity we define $\tau_{FF'} = -\sqrt{2}\lambda_{FF'}T_1^1(FF')$. With the help of Eq. (5) we first calculate the drift term of $|\psi\rangle\langle\psi'|$.

$$d(|\psi\rangle\langle\psi'|)_D = |d\psi\rangle_D\langle\psi'| + |\psi\rangle\langle d\psi'|_D + |d\psi\rangle_D\langle d\psi'|_D$$

$$= \sum_j\left(\langle L_j^\dagger\rangle_\psi L_j - \frac{1}{2}\langle L_j^\dagger\rangle_\psi\langle L_j\rangle_\psi - \frac{1}{2}L_j^\dagger L_j\right)|\psi\rangle\langle\psi'|$$

$$+ \sum_j|\psi\rangle\langle\psi'|\left(\langle L_j\rangle_{\psi'}L_j^\dagger - \frac{1}{2}\langle L_j^\dagger\rangle_{\psi'}\langle L_j\rangle_{\psi'}\right.$$

$$\left. -\frac{1}{2}L_j^\dagger L_j\right) + \sum_j(L_j - \langle L_j\rangle_\psi)|\psi\rangle\langle\psi'|(L_j^\dagger - \langle L_j^\dagger\rangle_{\psi'}).$$

(8)

The third term in the above comes from the product of the fluctuation terms of Eq. (5) proportional to $d\xi_i d\xi_j^*$, which for $i \neq j$ is of order higher than dt and therefore negligible, but for $i=j$ is a deterministic drift term of order dt. Using Eq. (8) we can now compute the drift term of the operators $\tau_{FF'}$. Their evolution is strictly determined by four coupled equations. We will however, neglect the influence of the fast precessing hyperfine coherences τ_{ab} and τ_{ba} and consider only the low frequency coherences τ_{FF} with $F=a,b$. After some algebra we find, by also including the Hamiltonian evolution as well as the fluctuation terms, that

$$d\boldsymbol{\tau} = -dt\left(\frac{K}{T_2} + i\Omega\right)\boldsymbol{\tau} + \frac{\Xi}{\sqrt{T_2}}d\boldsymbol{\xi},$$

(9)

where $\boldsymbol{\tau} = (\langle\tau_{aa}\rangle \ \langle\tau_{bb}\rangle)^T$, the drift matrix is

$$K = \begin{pmatrix} \dfrac{[I]^2 - [I] + 1}{2[I]^2} & \dfrac{[I]^2 + 3[I] + 2}{2[I]^2} \\ \dfrac{[I]^2 - 3[I] + 2}{2[I]^2} & \dfrac{[I]^2 + [I] + 1}{2[I]^2} \end{pmatrix},$$

(10)

with $[I] = 2I+1$, the Hamiltonian matrix is

$$\Omega = \begin{pmatrix} \omega_L & 0 \\ 0 & -\omega_L \end{pmatrix}$$

with $\omega_L = g_s\mu_B B/\hbar[I]$ being the Larmor frequency, and $d\boldsymbol{\xi} = (d\xi_a \ d\xi_b)^T$ with $d\xi_a$ and $d\xi_b$ being two real and independent Wiener processes with unit diffusion constant [26]. This means, for example, that $d\xi_a(t) = N(t)\sqrt{dt}$, where $N(t)$ is a normal random variable with zero mean and unit variance. Finally, the fluctuation matrix is found to be

$$\Xi = \begin{pmatrix} \sqrt{\dfrac{[I]^4 + 5[I]^3 + 10[I]^2 + 10[I] + 4}{240[I]^5}} & 0 \\ 0 & \sqrt{\dfrac{[I]^4 - 5[I]^3 + 10[I]^2 + 20[I] + 4}{240[I]^5}} \end{pmatrix}. \tag{11}$$

The above stochastic evolution equation of the vector $\boldsymbol{\tau}$ is thus a bivariate Ornstein-Uhlenbeck process [26] and in the long-time limit it is described in the frequency domain by a power spectral density function [27]

$$S(\omega) = \frac{1}{2\pi T_2}\left[\frac{K}{T_2} + i(\Omega + \omega)\right]^{-1} \Xi\Xi^T \left[\frac{K^T}{T_2} - i(\Omega + \omega)\right]^{-1}. \tag{12}$$

In Fig. 1 we plot the trace of the power spectrum matrix $S(\omega)$ for the case of ^{85}Rb ($I=5/2$). The heights of the spin-noise resonance peaks of the upper and lower hyperfine multiplets, appearing at $-\omega_L$ and ω_L, respectively, are determined by the total noise power and the respective decay rates. These are given in terms of the diagonal elements of the fluctuation and drift matrix, respectively. They are both affected by the hyperfine level multiplicity, leading to a stronger spin-noise resonance of the upper hyperfine multiplet. Considering only positive frequencies from now on, it easily follows that the power spectrum of the observable $\langle s_y \rangle$ will be given by

$$\mathcal{F}_{\mathrm{PSD}_{\langle s_y \rangle}}(\omega) = \frac{\mathrm{Tr}\{S(\omega) + S(-\omega)\}}{2}, \tag{13}$$

which for $\omega_L \gg 1/T_2$ can be approximately written as

$$\mathcal{F}_{\mathrm{PSD}_{\langle s_y \rangle}}(\omega) = \frac{1}{4\pi}\sum_{i=1}^{2} \frac{\Xi_{ii}^2/T_2}{(\omega - \omega_L)^2 + (K_{ii}/T_2)^2}. \tag{14}$$
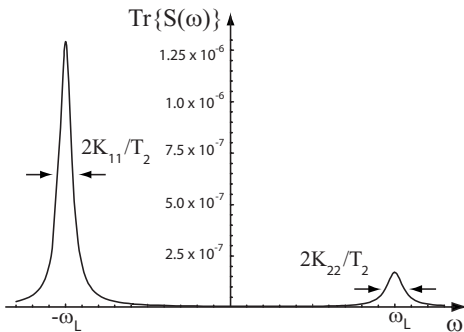

FIG. 1. Calculated noise spectrum $\mathrm{Tr}\{S(\omega)\}$, in units of Hz^{-1}, for $\omega_L = 10^4 \times \mathrm{s}^{-1}$, $1/T_2 = 0.1\omega_L$ and $I = 5/2$. The noise peaks of both hyperfine multiplets can be approximated by Lorentzians with half widths given, in terms of $1/T_2$, by the diagonal elements of the drift matrix K.

B. Stochastic evolution of the paramagnetic Faraday rotation angle

In the experimental arrangement we will be considering in the following, a linearly polarized and off-resonant probe laser interacts with the unpolarized alkali-metal vapor. The effect of the atoms on the light is described by the polarizability tensor, which is an operator acting on the ground states of the atoms. If we write $\Delta = \delta + i\gamma_c/2$, where $\delta = \omega - \omega_0$ is the detuning and γ_c is the FWHM of the optical absorption line due to collisions with buffer gas atoms, then the polarizability is given to first order in $1/\Delta$ by [28]

$$\alpha = -\frac{1}{\hbar}\frac{\mathbf{D}_{ge}\mathbf{D}_{eg}}{\Delta}, \tag{15}$$

where $\mathbf{D}_{ge} = P_g \mathbf{d} P_e$ and $\mathbf{D}_{eg} = P_e \mathbf{d} P_g$ with P_g and P_e being the projection operators to the ground and excited state manifold, respectively, and $\mathbf{d}$ the electric dipole moment operator. By use of the tensor operator formalism, it can be shown [29] that α can be decomposed into a scalar and a vector part

$$\alpha = -\alpha_0 + 4\alpha_0 s_y S_y, \tag{16}$$

where $\alpha_0 = r_e \lambda^2 \omega_0 f_{D2}/8\pi^2 \Delta$, $S_y = (\mathbf{x}_1 \mathbf{x}_1^{\dagger} - \mathbf{x}_{-1}\mathbf{x}_{-1}^{\dagger})/2$ is the $\hat{\mathbf{y}}$ component of the Poincaré spin describing the photon polarization, $\mathbf{x}_{\pm 1} = \mp(\hat{\mathbf{z}} \pm i\hat{\mathbf{x}})/\sqrt{2}$, r_e is the classical electron radius, and f_{D2} is the $D2$-transition oscillator strength. The eigenpolarizations of α are $\mathbf{x}_{\pm 1}$ with corresponding eigenvalues $\pm 1/2$. Thus the refraction index for $\sigma^{\pm}$ light will be $n_{\pm} = 1 - 2\pi[N]\alpha_0(1 \mp 2s_y)$, where $[N]$ is the alkali-metal atom number density. The Faraday rotation angle θ induced by one atom in the measurement volume is then given by

$$\theta = \pi(n_+ - n_-)\frac{l}{\lambda} = \frac{8\pi^2\alpha_0}{A\lambda}s_y \equiv \theta_0 s_y, \tag{17}$$

where l and Al are the length and volume of the vapor, respectively, probed by the laser. Taking into account the fact that the resonant absorption cross section for a $J=1/2 \rightarrow J' = 3/2$ transition with radiative width γ and total width γ_c is [30] $\sigma_0 = \frac{\lambda^2}{\pi}\frac{\gamma}{\gamma_c}$ and the integrated absorption cross section is $\int \sigma(\omega)d\omega = 2\pi^2 c r_e f_{D2}$, we can write (for $\delta \gg \gamma_c$)

$$\theta = \theta_0 s_y, \quad \theta_0 = \frac{1}{2\pi}\frac{\lambda^2}{A}\frac{\gamma}{\delta}. \tag{18}$$

Accordingly, the fluctuations of $\langle s_y \rangle$ will appear in the fluctuations of $\langle \theta \rangle$, as well as of $\langle \Theta \rangle = \theta_0 \sum_{i=1}^{N}\langle s_y^{(i)} \rangle$, which is the measured Faraday rotation angle resulting from the uncorrelated contributions of N atoms probed by the laser beam,
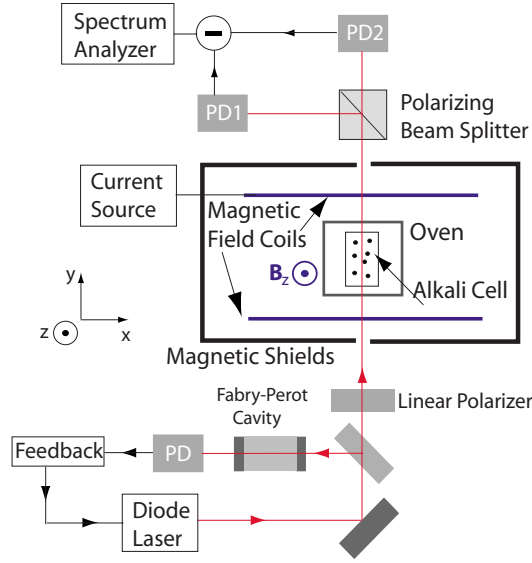
FIG. 2. (Color online) Experimental scheme for low-field spin-noise measurement. PD stands for photodiode.

where $s_y^{(i)}$ is the $\hat{\mathbf{y}}$ component of the (i)th atom's spin. The power spectral density of $\langle \Theta \rangle$ will then be

$$\mathcal{F}_{\text{PSD}_{\langle \Theta \rangle}}(\omega) = N\theta_0^2 \mathcal{F}_{\text{PSD}_{\langle s_y \rangle}}(\omega). \quad (19)$$

For an order-of-magnitude estimate of the spin-noise-induced rotation angle noise, we find that for the operating detuning and probe laser beam area (see Sec. III for the numerical values) $\theta_0 \approx 10^{-11}$ rad. Furthermore, based on Eq. (13) and Fig. 1, we find that the fluctuations of $\langle s_y \rangle$, δs_y, are on the order of $10^{-3}/\sqrt{\text{Hz}}$. Therefore, for $N=10^{12}$ atoms, the fluctuations of Θ should be $\delta\Theta = \sqrt{N}\theta_0 \delta s_y \approx 10$ nrad$/\sqrt{\text{Hz}}$, which is roughly at the level of photon shot noise limited rotation angle noise, and consistent with our measurements as described in the following.

III. EXPERIMENT

The experimental setup used for our measurements of spin noise is depicted in Fig. 2. We use a cylindrical glass cell (2 cm diameter, 2 cm inside length) filled with rubidium metal of natural isotopic abundance and with 300 torr of nitrogen buffer gas to suppress transit-time broadening. The cell is located in an oven heated by hot air flow to temperatures in the range of 80–120 °C. The oven with the cell reside inside a magnetic shield apparatus, which contains coils for the application of the desired magnetic fields. A static magnetic field is needed in order to shift the spin-noise spectrum to a frequency range void of technical noise sources. The Faraday rotation angle noise spectrum is peaked at the Larmor frequency, which is 25 kHz for an applied field $B_z = 53.6$ mG. The probe laser, an external cavity diode laser (New Focus 6224) with an elliptical beam profile of FW1/e dimensions of 0.6×2.3 mm (measured with a CCD camera), is red detuned by 45 GHz from the $D2$ resonance. The laser frequency is actively locked at the desired detuning with a Fabry-Pérot cavity. Before entering the cell, the laser is po-
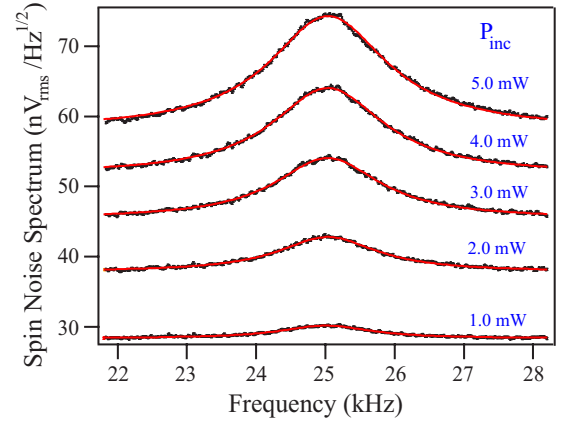

FIG. 3. (Color online) Spin-noise spectra at $T=120.5$ °C, for various values of the incident probe laser power. The black points are measured data and the line is the fit (see the text for the functional form).

larized at 45° with respect to the $\hat{\mathbf{z}}$ axis. The rotation of the probe laser polarization after traversing the cell is measured with a balanced polarimeter, which feeds the input of the spectrum analyzer, which is set at a frequency span of 6.4 kHz with an 8 Hz frequency bin width. Each spectrum was averaged for about 30 min. The measured signal V has a power spectral density, in units of V^2/Hz, given by

$$\mathcal{F}_{\text{PSD}_V}(\omega) = (2P_t r R_L)^2 [\mathcal{F}_{\text{PSD}_{\langle \Theta \rangle}}(\omega) + (\delta\phi)^2] + V_e^2, \quad (20)$$

where P_t is the transmitted probe laser power, $r \approx 0.5$ mA/mW is the photodiode responsivity, and $R_L = 3.9$ kΩ is the photodiode load resistor. The term in Eq. (20) involving $\delta\phi$ represents the photon shot noise, where $\delta\phi \sim 1/2\sqrt{\dot{N}}$ is the rotation angle measurement shot noise limit [30] after counting $\dot{N}\tau$ photons in a measurement time τ, with $\dot{N}=P_t/(hc/\lambda)$ being the photon flux. The photon shot noise dominates the background noise of the spectra shown in Fig. 3, as can be verified from the scaling of the background with $\sqrt{P_{inc}}$, where P_{inc} is the incident probe laser power. A dark electronic background of $V_e=16$ nV$/\sqrt{\text{Hz}}$ is also present. We have verified that the integrated noise power of the Lorentzian spin-noise spectrum scales as [Rb], where [Rb] is the rubidium number density, as should be the case for spin-noise signals from uncorrelated atoms. This is shown in Fig. 4(a).

IV. DATA ANALYSIS

The total half-width of the spin resonance $\Gamma/2$ is given by

$$\Gamma/2 = \alpha K_{11}(1/T_{\text{se}} + 1/T_{\text{sd}}) + \gamma_{\text{trans}}, \quad (21)$$

where γ_{trans} is the transit time broadening due to the finite interaction time with the probe beam (the relaxation rate due to the diffusion of the alkali-metal atoms to the depolarizing cell walls is negligible). The correction factor $\alpha=1.038$ comes about as follows. The quadratic Zeeman effect shifts the Larmor frequency of the lower hyperfine manifold by 45 Hz at our operating magnetic field. Furthermore, the
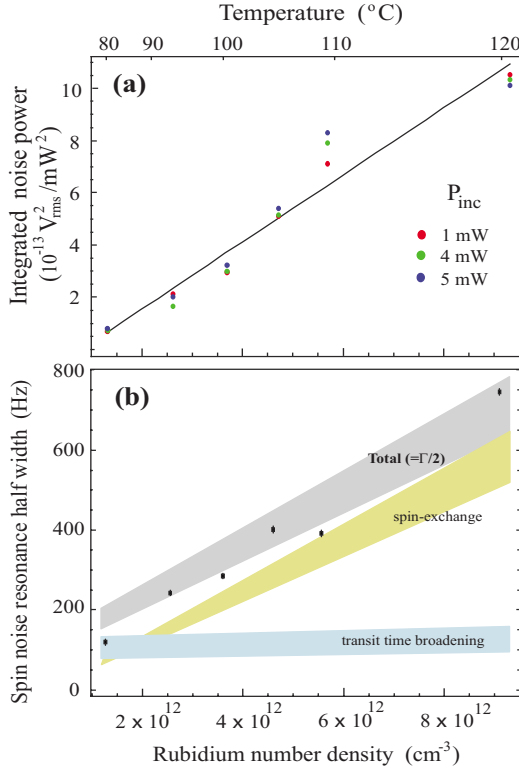
FIG. 4. (Color online) (a) Integrated spin-noise power (normalized by P_t) for three different values of the incident laser power with linear fit and (b) measured spin-noise resonance half-widths, superimposed on the calculation based on Eq. (22), versus rubidium number density.

Lorentzian power spectrum is approximate. We thus use the exact result of Eq. (13) and fit it with a single Lorentzian. The half-width of the latter is $\alpha K_{11}/T_2$. The spin-exchange cross section is $\sigma_{se}=2\times10^{-14}$ cm^2, whereas the spin-destruction cross sections for Rb-Rb and Rb-N$_2$ collisions are [31] $\sigma_{sd}^{Rb\text{-}Rb}=9\times10^{-18}$ cm^2 and [32] $\sigma_{sd}^{Rb\text{-}N_2}=1\times10^{-22}$ cm^2, respectively. It is clear that for our operating parameters, the contribution of Rb-Rb spin-destruction collisions to transverse relaxation is negligible and will not be considered henceforth. The transit time broadening is [33] $\gamma_{trans}=5.8D/R^2$, where $R=\sqrt{r_1 r_2}$ is the geometric mean of the probe laser beam elliptical profile dimensions and $D=D_0(p_0/p)(T/T_0)^{3/2}$ is the Rb-N$_2$ diffusion coefficient with [32] $D_0=0.28$ cm^2/s, $p_0=760$ torr, $T_0=424$ °K, p the nitrogen pressure, and T the cell temperature. The error of γ_{trans} is estimated [34] to be at the 20% level. All together, the half-width $\Gamma/2$ will be

$$\Gamma(T)/2 = \alpha K_{11}(\sigma_{se}\bar{v}_{Rb\text{-}Rb}[Rb] + \sigma_{sd}^{Rb\text{-}N_2}\bar{v}_{Rb\text{-}N_2}[N_2]) + 5.8D/R^2,$$
(22)

where the temperature dependence of $\Gamma/2$ stems from the temperature dependence of the average relative velocities $\bar{v}_{Rb\text{-}Rb}$ and $\bar{v}_{Rb\text{-}N_2}$, the diffusion coefficient D, and the rubidium number density [Rb]. In Fig. 3 we show measured spin-noise spectra for a specific temperature and for various values of the incident probe laser power. For each of these

values, the spin-noise signal (in units of nV/$\sqrt{\text{Hz}}$) is fitted to a function of the form $\sqrt{a+\frac{b}{(f-f_o)^2+(\gamma/2)^2}}$ from which the HWHM $\gamma/2$ is extracted. The actual half-width $\Gamma/2$ for that temperature is found by a linear extrapolation to zero probe laser power in order to eliminate the contribution of optical pumping. From the linear dependence of the half-width on intensity, we find that optical pumping adds 45–80 Hz/mW to $\Gamma/2$, depending on temperature, in rough agreement with $R=50$ Hz/mW found by using the expression $R=(1/2\pi)\int\Phi(\nu)\sigma(\nu)d\nu$, where $\Phi(\nu)$ is the photon flux and $\sigma(\nu)$ the optical absorption cross section. In Fig. 4(b) we show the measured spin-noise resonance half-widths, superimposed on the spin-relaxation rates stemming from the various terms of Eq. (22), together with their error bands, as well as the total rate, versus the number density of rubidium. The latter was measured by a combination of absorption spectroscopy and Faraday rotation [28] at a longitudinal magnetic field $B_y=55$ G and was found to be smaller than that predicted by the Killian formula [35], probably due to the treatment of the specific glass (pyrex) cell. Specifically, we calibrated the Faraday rotation spectra at low temperatures (70–80 °C) by absorption measurements and used this calibration at the higher temperatures. This was done in order not to be dependent on the near-resonant line shape of the Faraday rotation angle, since the operating detuning was limited by the mode-hop-free scanning range of our diode laser around the $D2$ resonance (60 GHz).

V. CONCLUSIONS

We have shown that spin-relaxation rates in alkali-metal vapors can be extracted in a nonperturbative way by an off-resonant probe laser sensitive to the spin fluctuations of the alkali-metal vapor. The extracted rates are consistent with the known rates, to within 10%, limited by the uncertainty in rubidium number density. This method could also be used to directly measure relaxation rates due to anisotropic interactions in alkali-metal collisions with noble gas atoms. This could be accomplished by extending the previous single channel measurement to a measurement of spatiotemporal correlations of the spin-noise signals induced into the polarization of two different probe beams. Such correlations will essentially contain a selectively enhanced contribution of certain collision histories of the Rb atoms to spin relaxation, i.e., they will contain a nonzero collisional average $\langle(\mathbf{r}\cdot\mathbf{S})(\mathbf{r}\cdot\mathbf{K})\rangle$, where $\mathbf{S}$ and $\mathbf{K}$ are the alkali-metal electron spin and the noble gas atom nuclear spin, respectively, and $\mathbf{r}$ is the vector joining the nuclei of the two collision partners. Accordingly, long trajectories, in which such a collisional average will tend to zero, will be suppressed by $e^{-\tau/T_2}$, where τ is the alkali-metal atom diffusion time from one probe beam to the other. The relaxation rate due to anisotropic interactions in Rb–^{3}He collisions is calculated [36] to be about 3% of the total Rb spin destruction rate due to Rb–^{3}He collisions. At the magnetic field used for this work, the latter would amount to about 10% of the total transverse relaxation rate, rendering the anisotropic contribution negligible. However, by working at an even lower magnetic field and higher

Rb densities, one can enter the regime of suppression of the spin-exchange relaxation [37]. For example, for [Rb] $\approx 10^{14}$ cm^{-3}, and $\omega_L \approx 2\pi \times 1$ kHz, it follows [38] that the spin-exchange relaxation rate will have been suppressed to $\gamma_{se} \approx 2\pi \times 25$ Hz, in which case the anisotropic rate would amount to a few percent of the total relaxation rate. To single out anisotropic rates from different kinds of correlations would, however, still require a challenging precision of the width extraction at the percent level.

[1] V. B. Braginsky and F. Y. Khalili, *Quantum Measurement* (Cambridge University Press, Cambridge, 1995).

[2] J. C. Allred, R. N. Lyman, T. W. Kornack, and M. V. Romalis, Phys. Rev. Lett. **89**, 130801 (2002).

[3] I. K. Kominis, J. C. Allred, T. W. Kornack, and M. V. Romalis, Nature (London) **422**, 596 (2003).

[4] M. Auzinsh *et al.*, Phys. Rev. Lett. **93**, 173002 (2004).

[5] I. M. Savukov, S. J. Seltzer, M. V. Romalis, and K. L. Sauer, Phys. Rev. Lett. **95**, 063004 (2005).

[6] T. W. Kornack, R. K. Ghosh, and M. V. Romalis, Phys. Rev. Lett. **95**, 230801 (2005).

[7] G. Katsoprinakis, D. Petrosyan, and I. K. Kominis, Phys. Rev. Lett. **97**, 230801 (2006).

[8] W. M. Itano *et al.*, Phys. Rev. A **47**, 3554 (1993).

[9] J. L. Sørensen, J. Hald, and E. S. Polzik, Phys. Rev. Lett. **80**, 3487 (1998).

[10] J. Hald, J. L. Sørensen, C. Schori, and E. S. Polzik, Phys. Rev. Lett. **83**, 1319 (1999).

[11] J. M. Geremia, J. K. Stockton, and H. Mabuchi, Science **304**, 270 (2004).

[12] R. Kubo, Rep. Prog. Phys. **29**, 255 (1966).

[13] F. Bloch, Phys. Rev. **70**, 460 (1946).

[14] T. Sleator, E. L. Hahn, C. Hilbert, and J. Clarke, Phys. Rev. Lett. **55**, 1742 (1985).

[15] N. Müller and A. Jerschow, Proc. Natl. Acad. Sci. U.S.A. **103**, 6790 (2006).

[16] T. Mitsui, Phys. Rev. Lett. **84**, 5292 (2000).

[17] E. B. Aleksandrov and V. S. Zapasskii, Sov. Phys. JETP **54**, 64 (1981).

[18] S. A. Crooker, D. G. Rickel, A. V. Balatsky, and D. L. Smith, Nature (London) **431**, 49 (2004).

[19] B. Mihaila *et al.*, Phys. Rev. A **74**, 043819 (2006).

[20] Z. Nussinov, M. F. Crommie, and A. V. Balatsky, Phys. Rev. B **68**, 085402 (2003).

[21] M. Oestreich, M. Römer, R. J. Haug, and D. Hägele, Phys. Rev. Lett. **95**, 216603 (2005).

[22] W. Happer, Rev. Mod. Phys. **44**, 169 (1972).

[23] N. Gisin and I. C. Percival, J. Phys. A **25**, 5677 (1992).

[24] S. Appelt *et al.*, Phys. Rev. A **58**, 1412 (1998).

[25] I. Percival, *Quantum State Diffusion* (Cambridge University Press, Cambridge, 1998).

[26] D. T. Gillespie, Am. J. Phys. **64**, 225 (1996).

[27] C. W. Gardiner, *Handbook for Stochastic Methods* (Springer-Verlag, Berlin, 1990).

[28] Z. Wu, M. Kitano, W. Happer, M. Hou, and J. Daniels, Appl. Opt. **25**, 4483 (1986).

[29] W. Happer and B. S. Mathur, Phys. Rev. **163**, 12 (1967).

[30] D. Budker, D. K. Kimball, and D. P. DeMille, *Atomic Physics* (Oxford University Press, Oxford, 2004).

[31] A. B.-A. Baranga *et al.*, Phys. Rev. Lett. **80**, 2801 (1998).

[32] M. E. Wagshul and T. E. Chupp, Phys. Rev. A **49**, 3854 (1994).

[33] J. E. M. Haverkort, H. G. C. Werij, and J. P. Woerdman, Phys. Rev. A **38**, 4054 (1988).

[34] J. Sagle, R. K. Namiotka, and J. Huennekens, J. Phys. B **29**, 2629 (1996).

[35] T. J. Killian, Phys. Rev. **27**, 578 (1926).

[36] D. K. Walter, W. Happer, and T. G. Walker, Phys. Rev. A **58**, 3642 (1998).

[37] W. Happer and A. C. Tam, Phys. Rev. A **16**, 1877 (1977).

[38] W. Happer and H. Tang, Phys. Rev. Lett. **31**, 273 (1973).